Front. Earth Sci. 2022, 16(2): 323–339
https://doi.org/10.1007/s11707-020-0862-9

RESEARCH ARTICLE

Estimation of bioclimatic variables of Mongolia derived from remote sensing data

Munkhdulam OTGONBAYAR (✉)[1], Clement ATZBERGER[2], Erdenesukh SUMIYA[3], Sainbayar DALANTAI[1], Jonathan CHAMBERS[4]

1 Institute of Geography and Geoecology, Mongolian Academy of Sciences (MAS), Ulaanbaatar 15170, Mongolia
2 Institute of Geomatics, University of Natural Resources and Life Sciences (BOKU), Vienna 1190, Austria
3 School of Arts and Sciences, National University of Mongolia (NUM), Ulaanbaatar 14201, Mongolia
4 Cooperazione Internazionale, Milan 50 20151, Italy

Abstract Global maps of bioclimatic variables currently exist only at very coarse spatial resolution (e.g. WorldClim). For ecological studies requiring higher resolved information, this spatial resolution is often insufficient. The aim of this study is to estimate important bioclimatic variables of Mongolia from Earth Observation (EO) data at a higher spatial resolution of 1 km. The analysis used two different satellite time series data sets: land surface temperature (LST) from Moderate Resolution Imaging Spectroradiometer (MODIS), and precipitation (P) from Climate Hazards Group Infrared Precipitation with Stations (CHIRPS). Monthly maximum, mean, and minimum air temperature were estimated from Terra MODIS satellite (collection 6) LST time series product using the random forest (RF) regression model. Monthly total precipitation data were obtained from CHIRPS version 2.0. Based on this primary data, spatial maps of 19 bioclimatic variables at a spatial resolution of 1 km were generated, representing the period 2002–2017. We tested the relationship between estimated bioclimatic variables (SatClim) and WorldClim bioclimatic variables version 2.0 (WorldClim) using determination coefficient (R^2), root mean square error (*RMSE*), and normalized root mean square error (*nRMSE*) and found overall good agreement. Among the set of 19 WorldClim bioclimatic variables, 17 were estimated with a coefficient of determination (R^2) higher than 0.7 and normalized RMSE (*nRMSE*) lower than 8%, confirming that the spatial pattern and value ranges can be retrieved from satellite data with much higher spatial resolution compared to WorldClim. Only the two bioclimatic variables related to temperature extremes (i.e., annual mean diurnal range and isothermality) were modeled with only moderate accuracy (R^2 of about 0.4 with *nRMSE* of about 11%). Generally, precipitation-related bioclimatic variables were closer correlated with WorldClim compared to temperature-related bioclimatic variables. The overall success of the modeling was attributed to the fact that satellite-derived data are well suited to generated spatial fields of precipitation and temperature variables, especially at high altitudes and high latitudes. As a consequence of the successful retrieval of the bioclimatic variables at 1 km spatial resolution, we are confident that the estimated 19 bioclimatic variables will be very useful for a range of applications, including species distribution modeling.

Keywords bioclimatic variables, MODIS land surface temperature, CHIRPS precipitation

1 Introduction

A large number of ecological studies have used climate-based models; two prominent examples are ecological niche models (Waltari et al., 2007; Feilhauer et al., 2012) and species distribution models (SDM) (Anderson, 2012). The United States Geological Survey (USGS) developed for such purposes climate indices, which can be referred to as bioclimatic variables (O'Donnell and Ignizio, 2012). The bioclimatic variables are widely used in species distribution modeling (Attorre et al., 2007; Waltari et al., 2014; Salas et al., 2017). SDMs integrate information on species appearance with environmental features to estimate their distributional range (Vega et al., 2018). SDMs are moreover valuable for other applications across evolutionary ecology and biology (Title and Bemmels, 2018).

Besides those applications, bioclimatic variables also capture features of climate (Mesquita and Sousa, 2009) that are directly related to plant physiologic processes

Received May 19, 2020; accepted January 5, 2021

E-mail: munkhdulamo@mas.ac.mn

determining primary productivity (Leathwick et al., 2003). The bioclimatic variables represent the types of seasonal trends relevant to the physiologic constraints of different species (O'Donnell and Ignizio, 2012). Bioclimatic variables also include information on annual conditions, as well as seasonal mean climate conditions and intra-year seasonality (O'Donnell and Ignizio, 2012; Fick and Hijmans, 2017). These variables represent annual trends, seasonality, and extreme or limiting environmental factors (Hijmans et al., 2005). Because of these characteristics, bioclimatic variables are widely used for vegetation mapping (Franklin, 1995; Hengl et al., 2018), and to study effects of climate change on species distribution for past, current and future scenarios (Sykes et al., 1996; Peng, 2000; Walther et al., 2005; O'Donnell and Ignizio, 2012), to monitor exotic and invasive species (Arriaga et al., 2004), for regional planning (Bryan and Crossman, 2008), ecosystem distribution (Thompson et al., 2004), and to assess drought risk (Incerti et al., 2007). At the global level, a set of 19 gridded data sets were developed within WorldClim based on weather stations, involving data from the Global Climate Network Data set (GHCN) (Lawrimore et al., 2011), the World Meteorological Organization climatological database, and additional minor database-specific weather stations (WMO, 2014). In WorldClim, the bioclimatic variables were derived from two climatic data sources to generate more biologically meaningful variables (O'Donnell and Ignizio, 2012), which are monthly mean, minimum, and maximum temperature, and monthly total precipitation.

There are two versions of WorldClim bioclimatic variables. WorldClim version 1.4 is a global climate gridded data set for the years 1961–1990 (excluding Antarctica) at 3 resolutions (2.5 min, 5 min, 10 min) (Hijmans et al., 2005; Marchi et al., 2019). WorldClim version 2.0 is a new data set containing grids with interpolated data from between 9000 and 60000 weather stations for 4 different spatial resolutions from 30 s (~1 km) to 10 min (~340 km) for the years 1971–2000 (Fick and Hijmans, 2017). In addition, Michael et al. (O'Donnell and Ignizio, 2012) developed a set of 20 bioclimatic variables as continuous raster surfaces between 1985 and 2009. Moreover, Vega et al. (2018) reproduced interpolation methods from WorldClim to create MERRAclim, a global set of 19 bioclimatic variables that includes Antarctica. MERRA (Modern Era Retrospective-analysis for Research and Application) is a NASA (National Aeronautics and Space Administration) atmospheric data reanalysis of satellite information. MERRAclim contains three data sets of 19 bioclimatic variables for the years 1980, 1990, 2000, using hourly temperature and humidity data from 1980 to 2000 at three different resolutions (2.5 min, 5 min, 10 min) (Vega et al., 2018).

In parallel, various large scale gridded interpolated temperature and precipitation data sets at different spatiotemporal resolutions have been developed from in situ measurements to estimate bioclimatic variables (Hijmans et al., 2005; Fick and Hijmans, 2017; Vega et al., 2018; Marchi et al., 2019). Unfortunately, in situ measured temperature and precipitation data with long temporal coverage are only available from a limited number of meteorological stations with inadequate spatial coverage (Otgonbayar et al., 2019). These data sets, therefore, suffer from uneven geographic coverage, with many areas of the Earth poorly represented (Hijmans et al., 2005).

On the contrary, EO satellites capture the entire Earth surface at much denser ground sampling distances (GSD) and with high temporal revisit frequency (usually 1 day). This data permits estimation of monthly mean, minimum, and maximum surface temperature (Benali et al., 2012), as well as monthly total precipitation (Sun et al., 2018). As sensor technology advances at a rapid pace, advanced geo-informatics techniques offer an opportunity to estimate monthly temperature more accurately, and collect precipitation data derived from remote sensing sensors such as multispectral imagery, radio detection ranging (RADAR), and light detection and ranging (Lidar) at different spectral, spatial, and temporal resolutions. For instance, Fick and Hijmans (2017) determined, satellite data enhanced by 5%–15% prediction quality of temperature variables, especially low spatial density areas. And improving the accuracy of precipitation data, they suggested using satellite-based precipitation data as covariates. Amiri et al. (2020) estimated 19 bioclimatic variables from temperature and precipitation instrumental records (Model 1), and remote sensing data (Model 2) at a resolution of 1 km during 2001–2017 in Isfahan province of Iran together with three topographic variables using five different regression models. Accuracy statistics in Model 2 was higher than Model 1. This study proved that bioclimatic variables derived from satellite were more effective. Our main goal is to explore alternative ways to improve temporal and spatial resolution of bioclimatic variables derived from remotely sensed data for species distribution modeling. This study specific aim was to estimate bioclimatic variables using time series of land surface temperature (LST) from Moderate Resolution Imaging Spectroradiometer (MODIS), and precipitation (P) from Climate Hazards Group InfraRed Precipitation with Station (CHIRPS) data and to apply the model to the entire land surface of Mongolia. For this analysis, we estimated monthly maximum, mean, and minimum air temperature from Terra MODIS satellite LST (MOD11A2) for period 2002−2017 using the random forest (RF) regression model and three predictors (Otgonbayar et al., 2019; Erdenedalai et al., 2020).

2 Study area

The study area covers the entirety of Mongolia (~1.566×10^6 km^2) and is shown in Fig. 1 together with some

environmental variables. The maps illustrate the spatial variability of the topography, climate, vegetation, and eco-region conditions. The land surface elevation is between 524 m and 4320 m above sea level (Fig. 1(a)). Of the total territory of Mongolia, 16.3% is < 1000 m above sea level, 43.6% 1000−1500 m, 22.6% 1500−2500 m, 11.6% 2500−3500 m, and 5.9% > 3500 m. According to the Köppen climate classification (Fig. 1(b)), the Mongolian climate ranges from dry (B) to continental (D). The annual mean temperature (Ta) ranges between −11.4°C and 9.6°C with strong temperature gradients (Fig. 1(c)). The temperature decreases continuously from the northwest to the south-east. Annual total precipitation ranges between 26 and 50 mm in the semi-desert and desert regions, and between 500 mm to 649 mm in the alpine meadow to tundra regions (Fig. 1(d)). The average above ground biomass as approximated by the normalized difference vegetation index (*NDVI*) increases gradually from south to north (Fig. 1(e)). Generally, *NDVI* is highly correlated with temperature and precipitation. In the terrestrial ecoregion world map (Olson et al., 2001), Mongolia is divided into 8 ecoregions from desert to tundra (Fig. 1(f)).

3 Data and method

3.1 Temperature data

Air temperature measurements from station data can in principle be interpolated to derive spatial maps (Robeson, 1994). However, interpolation errors are often significant, depending on local conditions and the spatial and temporal resolution of measured air temperature data and station density (Dodson and Marks, 1997). Similar to many other countries, Mongolia's weather station network for air temperature observations has insufficient spatial coverage.

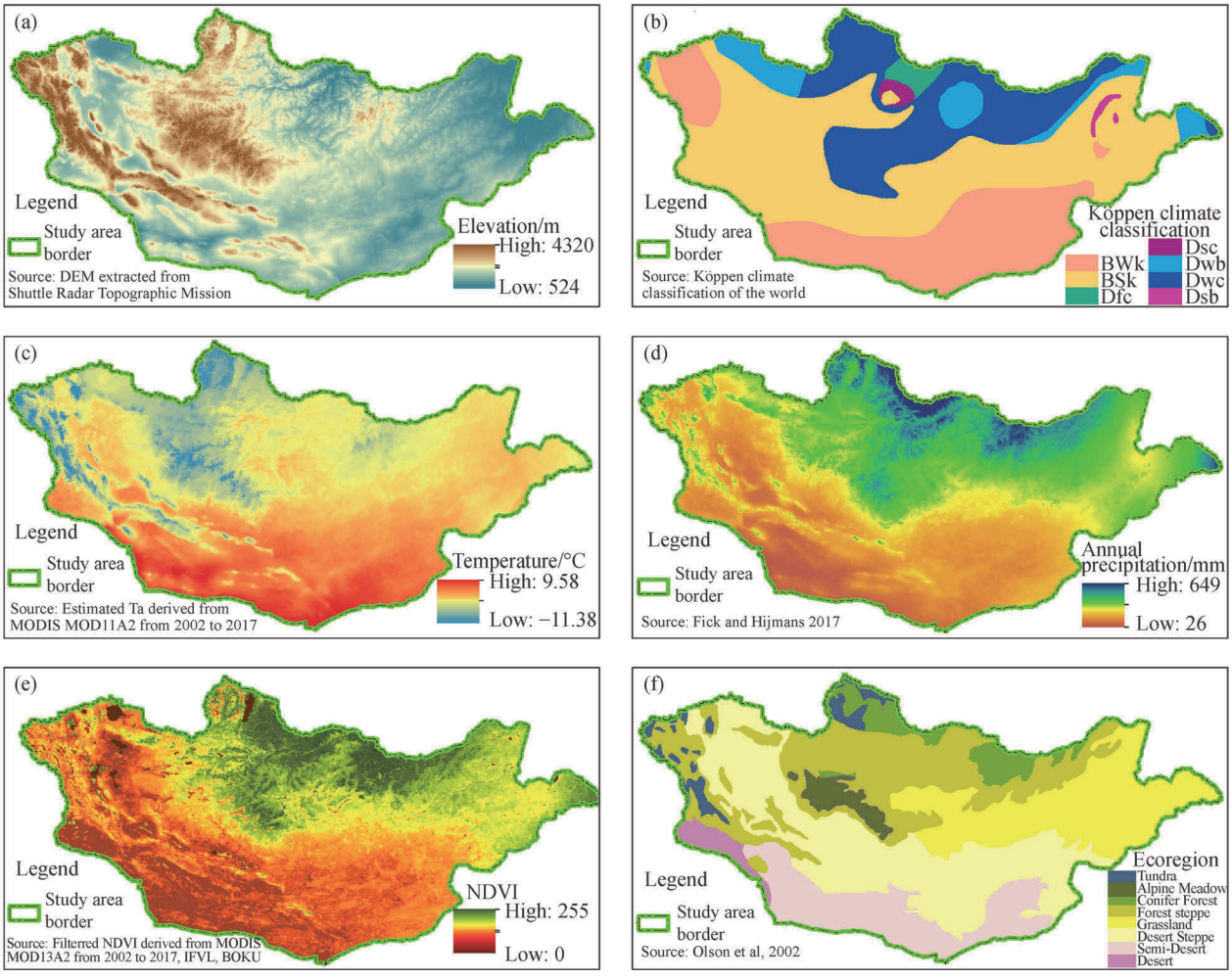

Fig. 1 Study area and important environmental variables. (a) Digital Elevation Model (DEM) derived from the Shuttle Radar Topography Mission (SRTM) with meteorological stations (n = 63), (b) Köppen climate classification of the world (Kottek et al., 2006), (c) estimated annual average air temperature derived from MODIS MOD11A2 (v006) (Otgonbayar et al., 2019), (d) annual total precipitation (Fick and Hijmans, 2017), (e) average annual NDVI derived from MODIS MOD13A2 (v006) (Vuolo et al., 2012), (f) Terrestrial Ecoregions of the World (Olson et al., 2001).

Satellite-derived land surface temperature (LST) data provide continuous spatial and temporal coverage and might, therefore, be used to model the temperature fields. However, satellites only measure land surface temperature (LST) and hence air temperature has to be estimated (Hooker et al., 2018). A suitable approach was presented in (Otgonbayar et al., 2019) where monthly maximum, minimum, and average air temperature over Mongolia was estimated using MODIS LST (MOD11A2, v006) time series and the random forest (RF) regression model. MODIS LST was obtained through an online data pool at the National Aeronautics and Space Administration (NASA) Land Processes Distributed Active Archive Centre (LP DAAC). Using the approach presented, we created spatial maps of monthly maximum temperature, minimum temperature (Erdenedalai et al., 2020), and average temperature (Otgonbayar et al., 2019) for the period of 2002−2017, at a spatial resolution of 1 km.

3.2 Precipitation data

Over the past two decades, numerous precipitation products have been generated from gauge-radar and gauge-satellite harmonized precipitation analysis at regional to global levels (Bai and Liu, 2018; Li et al., 2013; Price et al., 2014). Detailed information of the precipitation database combining rain gauge, satellite, and reanalysis products can be found for instance in Roca et al. (2019) and Beck et al. (2017). Here, we used two combined gauge-satellite data sets with a fine spatial resolution: CHIRPS and PERSIANN-CCS (Table 1). To select the most appropriate precipitation data, we compared CHIRPS and PERSIANN-CCS (see Appendix 1 for details). According to our findings (Table A1, Fig. A1), the CHIRPS data was overall far more accurate than PERSIANN-CCS. The main limitation of the CHIRPS data was its limited spatial coverage. Indeed, CHIRPS only covers the area 50°N–50°S whereas the northern part of Mongolia goes up to 52°N. To generate a gap-free wall-to-wall map for the entire territory of Mongolia, we filled the part of Mongolia between 50°N and 52°N with data from the Climate Hazards Center's Precipitation Climatology data version 1.0.

CHIRPS monthly total precipitation data sets were obtained from the Climate Hazard Center website with a spatial resolution 0.05°, spatial coverage 87°E−120E°, 41°N−50°N, and covering the period between 2002 and 2017. These data sets were developed in collaboration with scientists at the USGS Earth Resources Observation and Science (EROS), supported by the United States Agency for International Development's (USAID) Famine Early Warming Systems Network (FEWS NET). The data sets are built on 'smart' interpolation techniques, estimates focused on infrared Cold Cloud Duration (CCD) observations that are available in GeoTIFF, NetCDF, and BIL formats. The unit is mm per period, including mm per day, pentad, and month (Funk et al. 2015).

Here, we compared between derived from satellite (MODIS and CHRIPS) for period 2002–2017 and the weather station-based WorldClim data sets. WorldClim data sets include grids interpolated in situ station data for the 1970–2002 time period (Fig. 2). Estimated monthly maximum, mean, and minimum temperatures derived from MODIS LST are highly correlated with World Climatic temperature data sets compare to precipitation data sets (Table 2).

3.3 Methods

To calculate 19 bioclimatic variables at 1 km spatial resolution we used the functions listed in Table 3. The functions used as inputs satellite-derived air temperature (monthly maximum, monthly average, monthly minimum), and monthly total precipitation. Descriptive statistics for the 4 variables are provided in Table A2 and Fig. A2 (Appendix 2, Appendix 3). All calculations were done in R for statistical computing and graphics (Ripley 2001), and System for Automated Geoscientific Analyses (SAGA GIS) for analysis of spatial data (SAGA G, 2013). The analysis used the 'biovars' function of the 'dismo' package in R. To test the differences between our set of bioclimatic variables ("SatClim") and WorldClim bioclimatic variables, we used coefficient of determination (R^2), root mean squared error (*RMSE*), and normalized root mean squared error (*nRMSE*) as described in Table 4.

Table 1 Two precipitation products with a high spatial resolution (Roca et al., 2019; Sun et al., 2018; Bai and Liu, 2018; Beck et al., 2017). Only CHIRPS was used for this study. See Appendix 1 for a performance comparison

Product name	Acronym	Data used	Spatial coverage	Spatial resolution	Temporal coverage	Temporal resolution	Reference
Precipitation Estimation from Remotely Sensed Information using Artificial Neural Networks (PERSIANN)- Cloud Classification System	PERSIANN-CCS	Gauge- satellite	60°N–60°S	0.04°	2003– present	Hourly, Daily	Nguyen et al., 2018
Climate Hazards group Infrared Precipitation with Stations	CHIRPS v2.0	Gauge- satellite	50°N–50°S	0.05°	1981– present	Daily	Funk et al., 2015; Funk et al., 2015

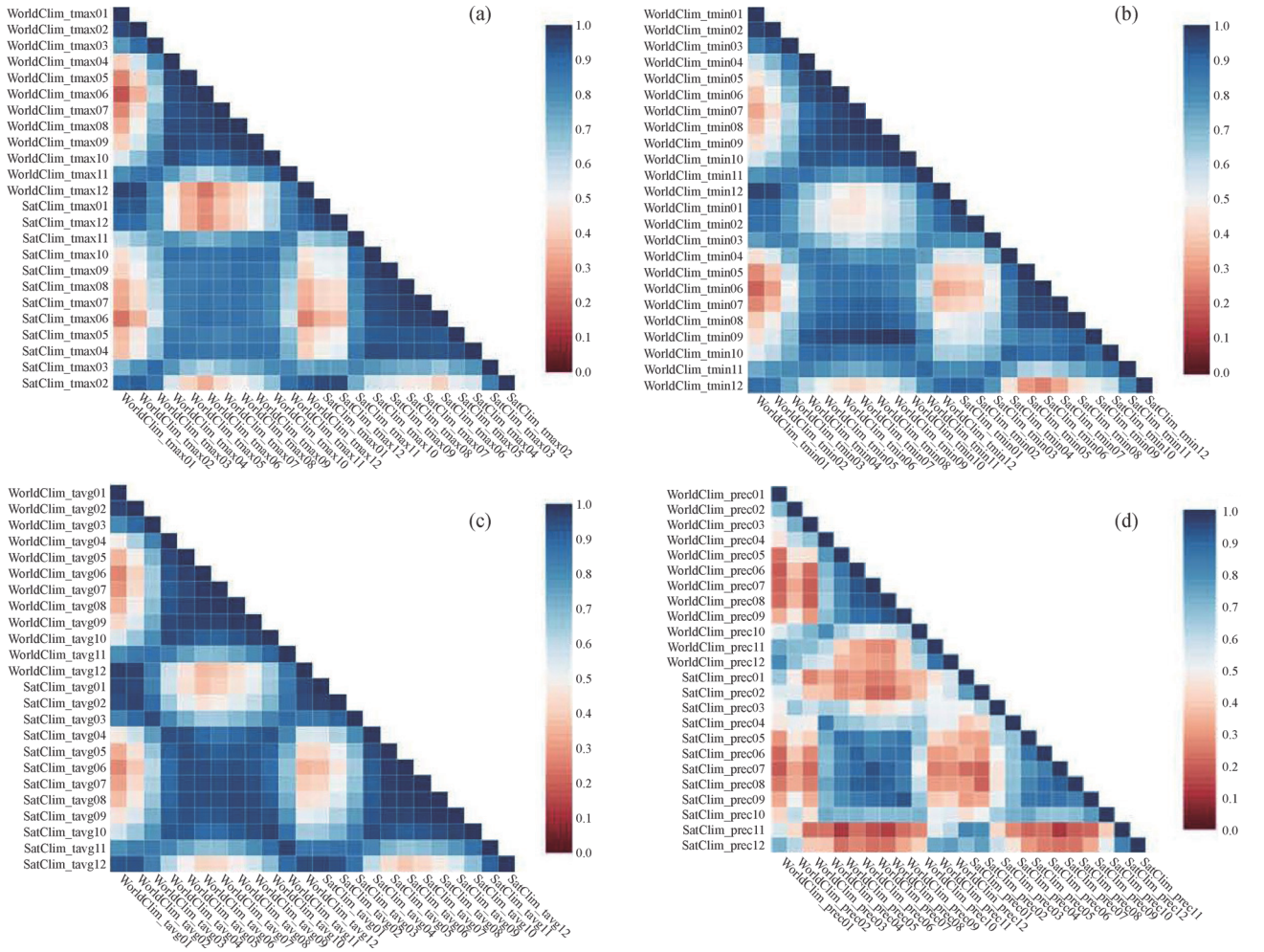

Fig. 2 Correlation matrix between WorldClim and SatClim four variables extracted from the metrological stations ($n = 63$). (a) monthly maximum temperature; (b) monthly minimum temperature; (c) monthly average temperature; (d) monthly total precipitation. High correlations were shown in blue and low correlations in red.

Table 2 Inter-correlation between estimated monthly air temperatures derived from MODIS LST, and World climatic data sets; precipitation CHRIPS and World climatic data sets ($n = 63$). High inter-correlations ($r \geqslant 0.90$) are highlighted in blue

Month	Maximum temperature/°C	Mean temperature/°C	Minimum temperature/°C	Total precipitation/mm
01	0.93	0.97	0.90	0.66
02	0.92	0.97	0.89	0.54
03	0.90	0.96	0.83	0.58
04	0.88	0.95	0.86	0.85
05	0.86	0.96	0.88	0.88
06	0.89	0.95	0.87	0.91
07	0.86	0.97	0.91	0.95
08	0.88	0.97	0.93	0.91
09	0.88	0.96	0.99	0.94
10	0.89	0.97	0.89	0.71
11	0.84	0.98	0.91	0.74
12	0.91	0.96	0.89	0.62

Table 3 Formula and description of the bioclimatic variables (O'Donnell and Ignizio, 2012). T_{avg}, T_{max}, and T_{min} are the monthly average, maximum and minimum air temperature, and PPT is the monthly total precipitation

Variable name	Unit	Formula	Description
Annual mean temperature	°C	$Bio\ 1 = \frac{\sum_{i=1}^{i=12} T_{avg_i}}{12}$	The annual mean temperature approximates the total energy for an ecosystem.
Annual mean diurnal range	°C	$Bio\ 2 = \frac{\sum_{i=1}^{i=12} (T_{max_i} - T_{min_i})}{12}$	Mean of the monthly temperature range. This variable can help provide information relating to the relevance of temperature variation for different species
Isothermality	%	$Bio\ 3 = \frac{Bio\ 2}{Bio\ 7} \times 100$	Isothermality quantifies how large the day to night temperatures fluctuate relative to the summer to winter (annual) fluctuations. A species distribution may be influenced by larger or smaller temperature oscillation within a month relative to the year and this variable is useful for confirming such information.
Temperature seasonality (Standard deviation)	°C	$Bio\ 4 = SD\{T_{avg_1},...,T_{avg_{12}}\}$	Temperature seasonality is a measure of temperature change over the year. A large Standard Deviation (SD) the larger variability of temperature.
Maximum temperature of the warmest month	°C	$Bio\ 5 = \max(\{T_{max_1} - T_{max_{12}}\})$	Monthly maximum temperature incidence over a given year (time series) or averaged span of years. This variable is useful to test that species distribution is affected influenced by warm temperature anomaly over the year.
Minimum temperature of the coldest month	°C	$Bio\ 6 = \min(\{T_{min_1} - T_{min_{12}}\})$	Monthly minimum temperature incidence over a given year (time series) or averaged span of years. This variable is useful to test that species distribution is affected influenced by cold temperature anomaly over the year.
Annual temperature range	°C	$Bio\ 7 = Bio\ 5 - Bio\ 6$	The measure of temperature fluctuation over a given year. This variable is useful to investigate whether species distribution is affected by the range of extreme temperature conditions.
Mean temperature of wettest quarter	°C	$Bio\ 8 = \frac{\sum_{i=1}^{i=3} T_{avg_i}}{3}\ or\ Q_{PPT_{max}}$	The quarterly variable is based on 3 months interval that is a mean temperature that prevails during the wettest season. The variable is useful for analyzing how such environmental factors can influence species season distribution.
Mean temperature of driest quarter	°C	$Bio\ 9 = \frac{\sum_{i=1}^{i=3} T_{avg_i}}{3}\ or\ Q_{PPT_{min}}$	The variable provides mean temperature during the driest 3 months of the year which is useful for analyzing how such environmental factors can influence species season distribution.
Mean temperature of warmest quarter	°C	$Bio\ 10 = \frac{\sum_{i=1}^{i=3} T_{avg_i}}{3}\ or\ Q_{T_{max}}$	The variable provides mean temperature during the warmest 3 months of the year which is useful for analyzing how such environmental factors can influence species season distribution.
Mean temperature of coldest quarter	°C	$Bio\ 11 = \frac{\sum_{i=1}^{i=3} T_{avg_i}}{3}\ or\ Q_{T_{min}}$	The variable provides mean temperature during the coldest 3 months of the year which is useful for analyzing how such environmental factors can influence species season distribution.
Annual precipitation	mm	$Bio\ 12 = \sum_{i=1}^{i=12} PPT_i$	The variable is recognized by the sum of 12 monthly precipitation values which is useful ascertaining the significance of water availability to the species distributions.
Precipitation of wettest month	mm	$Bio\ 13 = \max(\{PPT_1,...,PPT_{12}\})$	The variable is recognized by total precipitation values that prevail during the wettest month. The wettest month is useful if extreme precipitation conditions during the year affect a species potential range.
Precipitation of driest month	mm	$Bio\ 14 = \min(\{PPT_1,...,PPT_{12}\})$	The variable is recognized by total precipitation values that prevail during the driest month. The driest month is useful if extreme precipitation conditions during the year affect a species potential range.
Precipitation seasonality	mm	$Bio\ 15 = \frac{\mathrm{SD}(PPT_1,...,PPT_{12})}{1 + (Bio\ 12/12)}$	The variable is a measure of the variation monthly precipitation totals over the year. This variable is expressed by percentage where larger percentages represent greater variability of precipitation.
Precipitation of wettest quarter	mm	$Bio\ 16 = \max \sum_{i=1}^{i=3} PPT_i$	This quarterly provides total precipitation during the wettest 3 months of the year which can be useful for testing how such environmental factors can influence species season distribution.
Precipitation of driest quarter	mm	$Bio\ 17 = \min \sum_{i=1}^{i=3} PPT_i$	This quarterly provides total precipitation during the driest 3 months of the year which can be useful for testing how such environmental factors can influence species season distribution.
Precipitation of warmest quarter	mm	$Bio\ 18 = \sum_{i=1}^{i=3} PPT_i$ or $Q_{T_{max}}$	This quarterly provides total precipitation during the warmest 3 months of the year which can be useful for testing how such environmental factors can influence species season distribution.
Precipitation of coldest quarter	mm	$Bio\ 19 = \sum_{i=1}^{i=3} PPT_i$ or Q_{min}	This quarterly provides total precipitation during the coldest 3 months of the year which can be useful for testing how such environmental factors can influence species season distribution.

Table 4 Performance measures used in this study: coefficient of determination (R^2), root mean squared error (*RMSE*), and normalized RMSE (*nRMSE*). The three statistics represent correlation (association), error (residual), and range normalized errors (Richter et al., 2012)

Formula	Description	Range	Reference
$R^2 = 1 - \frac{\sum_{i=1}^{n} \left(V_{\text{est}}^{i} - \hat{V}_{\text{est}}\right)^2}{\sum_{i=1}^{n} \left(V_{\text{est}}^{i} - \overline{V}_{\text{est}}\right)^2}$	The R^2 measures the correlation between the predicted and observed value (fraction of explained variance)	0 to 1	Richter et al. (2012)
$RMSE = \sqrt{\frac{1}{n}\sum_{i=1}^{n} \left(V_{\text{est}}^{i} - V_{\text{obs}}^{i}\right)^2}$	The *RMSE* is a measure of the average magnitude of errors along the 1-to-1 line	Data unit	
$nRMSE = \frac{RMSE}{Range_{(\text{obs})}}$	Normalizing the *RMSE* facilitates the comparison between data sets or models with different scales. *nRMSE* is the ratio of the *RMSE* to the variance of the observed variable.	0 to ∞	Barzegar et al. (2016)

Notes: V_{est}^{i} – estimated variables, $\hat{V}_{\text{est}}$ – average of the estimated variables, $\overline{V}_{\text{est}}$ – average of the predicted variables, V_{obs}^{i} – observed variables, $Range_{(\text{obs})}$ – range of the observed variables and *n*-number of observed variables

4 Results

In Table 5, descriptive statistics of the estimated 19 bioclimatic variables are reported. Spatial maps of 19 bioclimatic variables at a spatial resolution of 1 km for the period 2002–2017 are shown in Fig. 3. In this figure we also provide a comparison between the estimated bioclimatic variables (SatClim) and WorldClim version 2. Results of the statistical analysis are reported in Table 6.

For almost all of the 19 SatClim and WorldClim bioclimatic variables, high correlations ($R^2 \geqslant 0.70$) were revealed in the linear regression between the $> 1.5 \times 10^6$ pairs of values. Only for the annual mean diurnal range (02) and Isothermality (03) we found lower – but still moderate – correlations ($R^2 \approx 0.40$–0.46). Only for these two variables the normalized *RMSE* (*nRMSE*) slightly exceeded 10%. The *nRMSE* of the remaining 17 bioclimatic variables were all below 8% (with six variables $nRMSE < 4\%$). The seven precipitation-related bioclimatic variables were generally more closely correlated with WorldClim compared to the 11 temperature-related bioclimatic variables (Table 6). Examining the consistency of retrieved frequency distribution (WorldClim versus SatClim), we found generally a very similar pattern, often characterized by multi-modal distributions (Fig. 3, last column).

Table 5 Descriptor statistics of the estimated 19 bioclimatic variables (SatClim) for the years 2002–2017 (n = 1 575 107 pixel)

Variables	Maximum	Mean	Minimum	Standard deviation
Annual mean temperature (01)	11.2	1.5	−13.4	3.6
Annual mean diurnal range (02)	12.6	7.3	4.4	1.0
Isothermality (03)	24.6	15.4	9.4	1.9
Temperature seasonality (04)	1960.0	1332.5	686.3	162.8
Maximum temperature of the warmest month (05)	32.2	22.3	−1.1	4.4
Minimum temperature of the coldest month (06)	−11.8	−25.4	−39.8	4.2
Annual temperature range (07)	64.4	47.7	28.3	4.9
Mean temperature of wettest quarter (08)	29.1	18.1	−3.2	4.4
Mean temperature of driest quarter (09)	2.9	−16.6	−31.0	4.9
Mean temperature of warmest quarter (10)	29.1	18.5	−3.2	4.5
Mean temperature of coldest quarter (11)	−7.6	−18.6	−32.0	4.2
Annual precipitation (12)	53.8	15.2	1.7	7.5
Precipitation of wettest month (13)	166.0	51.3	7.2	26.1
Precipitation of driest month (14)	10.0	1.5	0.0	0.8
Precipitation seasonality (15)	192.9	109.3	47.7	10.7
Precipitation of wettest quarter (16)	436.0	139.1	18.4	69.9
Precipitation of driest quarter (17)	30.0	5.3	0.0	2.6
Precipitation of warmest quarter (18)	436.0	133.7	12.3	70.7
Precipitation of coldest quarter (19)	53.6	6.1	0.0	3.1

Table 6 Summary of statistics describing the correspondence between SatClim and WorldClim data over Mongolia (R^2, *RMSE*, and *nRMSE*). For the comparison, 19 variables were extracted from the full image (n = 1 575 107 pixel). High correlations ($R^2 \geqslant 0.70$) are highlighted in light gray

Variable	R^2	*RMSE*	n*RMSE* (%)
Annual mean temperature (01)	0.97	0.61°C	2.48
Annual mean diurnal range (02)	0.46	0.95°C	11.57
Isothermality (03)	0.40	1.76%	11.59
Temperature seasonality (04)	0.86	61.14°C	4.80
Maximum temperature of the warmest month (05)	0.91	1.29°C	3.88
Minimum temperature of the coldest month (06)	0.76	2.05°C	7.31
Annual temperature range (07)	0.72	2.61°C	7.21
Mean temperature of wettest quarter (08)	0.95	1.00°C	3.10
Mean temperature of driest quarter (09)	0.70	2.69°C	7.95
Mean temperature of warmest quarter (10)	0.94	1.07°C	3.32
Mean temperature of coldest quarter (11)	0.93	1.32°C	5.43
Annual precipitation (12)	0.94	2.70 mm	5.19
Precipitation of wettest month (13)	0.90	8.13 mm	5.12
Precipitation of driest month (14)	0.73	0.54 mm	5.42
Precipitation seasonality (15)	0.76	8.50 mm	5.85
Precipitation of wettest quarter (16)	0.92	19.80 mm	4.74
Precipitation of driest quarter (17)	0.78	1.65 mm	5.50
Precipitation of warmest quarter (18)	0.87	2.20 mm	0.52
Precipitation of coldest quarter (19)	0.70	0.04 mm	3.64

Together, our results demonstrate that the spatial pattern, value ranges, and frequency distributions of WorldClim were generally well retrieved using the satellite derived inputs of SatClim. For the two variables annual mean diurnal range and isothermality, the lower correlations can be attributed to the fact that temperature extremes enter in the calculations; variables that are generally less well retrieved using satellite-based modeling techniques.

5 Discussion

Bioclimatic variables show information about annual conditions (e.g., 01, 02, 07, and 12), seasonal variations (e.g., 05, 06, 13, 14), and intra-year seasonality (e.g., 08–11, 16–19). These variables are represented as indicators relevant to the physiologic restrictions of species and are valuable for a number of applications (O'Donnell and Ignizio, 2012).

In recent years, at global level, bioclimatic variables mostly have been estimated from two commonly used types of data sets, namely WorldClim data sets (Fick and Hijmans, 2017; Marchi et al., 2019), and MERRAclim data sets (Vega et al., 2018). WorldClim version 1 and version 2 are global gridded data sets at a spatial resolution of ~1 km^2. WorldClim data sets are representative of the time period 1961–1990, and 1970–2000, respectively (Fick and Hijmans, 2017). WorldClim climate data sets, and bioclimatic variables are produced by geo-statistical interpolation methods (i.e., kriging and spline).

MERRAclim bioclimatic variables estimated from MERRAclim data sets, which are produced from station-based hourly data of air temperature, and specific humidity gridded data (instead of precipitation) from the Modern Era Retrospective Analysis for Research and Applications Reanalysis (MERRA) using a spline interpolation method for the years 1980, 1990, and 2000 (Vega et al., 2017). Therefore, MERRA data set is a climate reanalysis data set focused on weather station and modern remote sensing data. The disadvantage of MERRAclim bioclimatic variables with a coarse spatial resolution (10 arc-minutes, 5 arc-minutes, and 2.5 arc-minutes).

Moreover, several studies (Kurtzman and Kadmon, 1999; Brown and Comrie, 2002; Nikolova and Vassilev, 2006; Waltari et al., 2014) using various interpolation methods including kriging (co, simple, and ordinary), thin plate smoothing splines, and inverse distance weighting (IDW) to simultaneously on precipitation and temperature data sets had different level of success, and generally revealed larger errors for precipitation as compared to temperature (Mesquita and Sousa, 2009). Moreover, uncertainty of the interpolation-based method was increasing the time and asymmetry difference

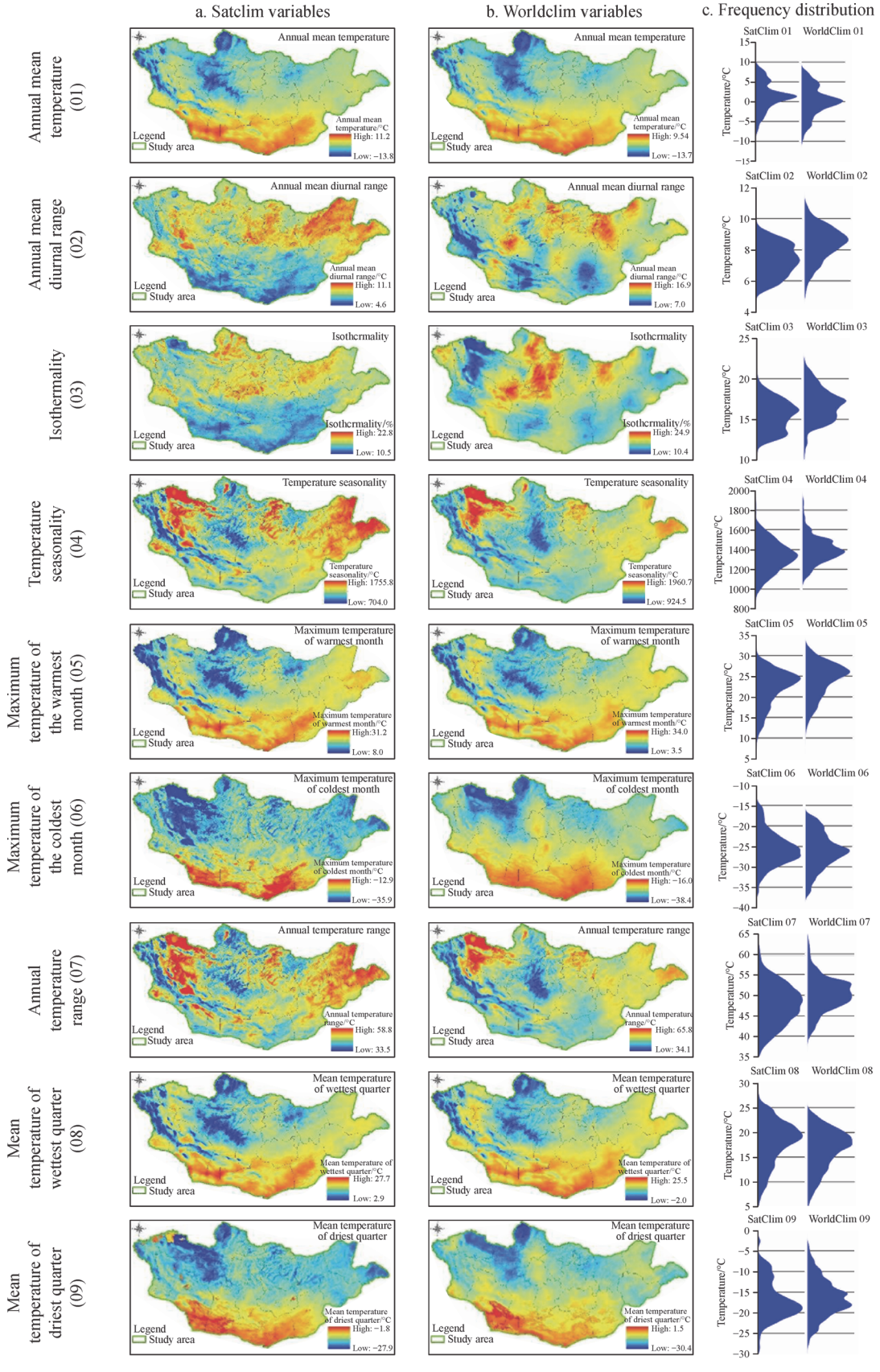
a. Satclim variables
b. Worldclim variables
c. Frequency distribution
Annual mean temperature (01)
Annual mean diurnal range (02)
Isothermality (03)
Temperature seasonality (04)
Maximum temperature of the warmest month (05)
Maximum temperature of the coldest month (06)
Annual temperature range (07)
Mean temperature of wettest quarter (08)
Mean temperature of driest quarter (09)
Legend
Study area
Annual mean temperature
Annual mean temperature/°C
High: 11.2
Low: −13.8
Annual mean temperature
Annual mean temperature/°C
High: 9.54
Low: −13.7
SatClim 01
WorldClim 01
Temperature/°C
Annual mean diurnal range
Annual mean diurnal range/°C
High: 11.1
Low: 4.6
Annual mean diurnal range
Annual mean diurnal range/°C
High: 16.9
Low: 7.0
SatClim 02
WorldClim 02
Temperature/°C
Isothermality
Isothermality/%
High: 22.8
Low: 10.5
Isothermality
Isothermality/%
High: 24.9
Low: 10.4
SatClim 03
WorldClim 03
Temperature/°C
Temperature seasonality
Temperature seasonality/°C
High: 1755.8
Low: 704.0
Temperature seasonality
Temperature seasonality/°C
High: 1960.7
Low: 924.5
SatClim 04
WorldClim 04
Temperature/°C
Maximum temperature of warmest month
Maximum temperature of warmest month/°C
High:31.2
Low: 8.0
Maximum temperature of warmest month
Maximum temperature of warmest month/°C
High: 34.0
Low: 3.5
SatClim 05
WorldClim 05
Temperature/°C
Maximum temperature of coldest month
Maximum temperature of coldest month/°C
High: −12.9
Low: −35.9
Maximum temperature of coldest month
Maximum temperature of coldest month/°C
High: −16.0
Low: −38.4
SatClim 06
WorldClim 06
Temperature/°C
Annual temperature range
Annual temperature range/°C
High: 58.8
Low: 33.5
Annual temperature range
Annual temperature range/°C
High: 65.8
Low: 34.1
SatClim 07
WorldClim 07
Temperature/°C
Mean temperature of wettest quarter
Mean temperature of wettest quarter/°C
High: 27.7
Low: 2.9
Mean temperature of wettest quarter
Mean temperature of wettest quarter/°C
High: 25.5
Low: −2.0
SatClim 08
WorldClim 08
Temperature/°C
Mean temperature of driest quarter
Mean temperature of driest quarter/°C
High: −1.8
Low: −27.9
Mean temperature of driest quarter
Mean temperature of driest quarter/°C
High: 1.5
Low: −30.4
SatClim 09
WorldClim 09
Temperature/°C

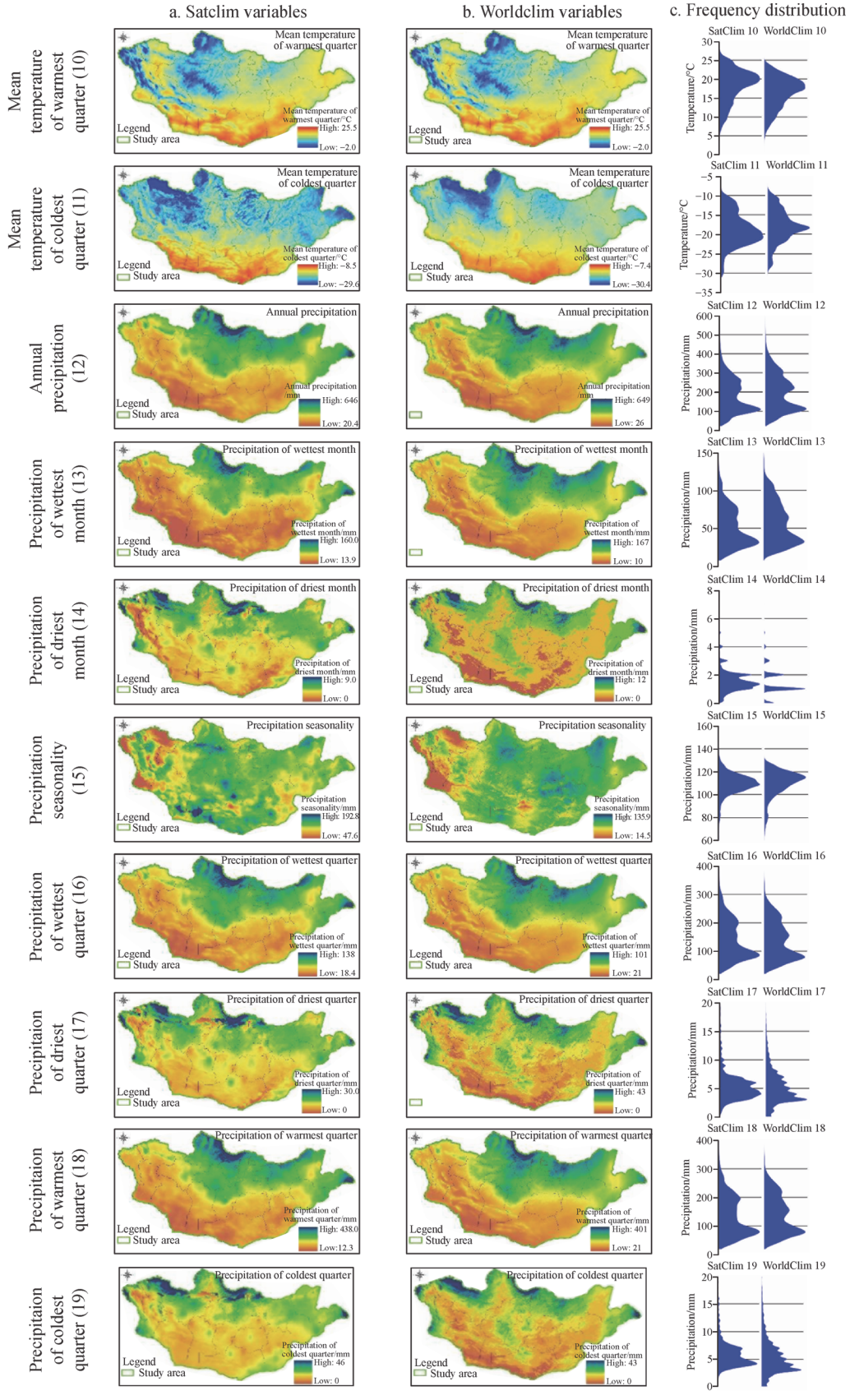

Fig. 3 (a) Modeled 19 SatClim bioclimatic variables using MODIS and CHIRPS data 2002–2017, (b) WorldClim variables with gridded data 1971–2000, (c) Frequency distributions of SatClim and WorldClim.

between future study and interpolation-based climate data sets (e.g., WorldClim) might lead to unsuitable predictions (Amiri et al., 2020). Conversely, satellite derived data are continuous in spatial and temporal coverage. Moreover, real-time access to satellite data have led to more up-to-date climate data (Amiri et al., 2020).

To remedy these limitations, we estimated bioclimatic variables (SatClim) using MODIS LST and CHIRPS data for the years 2002−2017. For this analysis, we estimated monthly maximum, mean, and minimum air temperature from Terra MODIS satellite LST (MOD11A2) for period 2002−2017 using the random forest (RF) regression model and three predictors (Otgonbayar et al., 2019; Erdenedalai et al., 2020). We examined the relationship between SatClim and WorldClim bioclimatic variables version 2.0 for the entire territory of Mongolia using the coefficient of determination (R^2), root mean squared error (*RMSE*), and normalized root mean squared error (*nRMSE*), which represent spatial correlation (association) and error (residual) (Richter et al., 2012).

In general, and considering WorldClim as a "reference", the spatial pattern of all 19 bioclimatic variables were well retrieved from MODIS and CHIRPS data and had moderate to highly positive correlations, with similar (often multi-modal) frequency distributions. The lower performance of the two variables annual mean diurnal range (02) and Isothermality (03) can be attributed to the fact that temperature extremes enter into their calculation. These temperature extremes are often underestimated using satellite-derived input data (Janatian et al., 2017; Duan et al., 2018; Hooker et al., 2018). Other 17 variables were estimated with normalized *RMSE* of $< 8\%$ with six of the 17 variables *nRMSE* $< 4\%$ (Table 6).

Amiri et al. (2020) estimated 19 bioclimatic variables from temperature and precipitation instrumental records (Model 1), and remote sensing data (Model 2) at a resolution of 1 km during 2001–2017 in Isfahan Province of Iran together with three topographic variables using five different regression models. Accuracy statistics in Model 2 was higher than Model 1. This study proved that bioclimatic variables derived from satellite were more effective.

The success of our satellite-derived method can be attributed to the fact that precipitation and temperature can be relatively well retrieved remotely (Kidd et al., 2010; Li et al., 2013; Funk et al., 2015; Beck et al., 2017; Paredes-Trejo et al., 2017; Sun et al., 2018), and especially in highly elevated or mountainous areas (Fick and Hijmans, 2017). In those areas, spatially and temporally continuous grids of land surface temperature (LST) are valuable inputs for accurate and robust air temperature retrievals with monthly resolution (Otgonbayar et al., 2019). In a similar way, by observing cloud top temperatures, it is possible to model monthly precipitation fields with relatively high accuracy (Bai and Liu, 2018). Without Earth Observation (EO) data, these primary variables have to be modeled and/or interpolated from sparse station data, often not capturing well local peculiarities (Vancutsem et al., 2010; Benali et al., 2012; Atzberger and Rembold, 2013).

6 Conclusions

Spatial maps of 19 bioclimatic variables at a spatial resolution of 1 km were generated for the entire territory of Mongolia, representing the period 2002–2017. The analysis used two different satellite time series data: MODerate Resolution Imaging Spectroradiometer (MODIS) land surface temperature (LST), and Climate Hazards Group Infrared Precipitation with Stations (CHIRPS). To estimate monthly maximum, mean, and minimum air temperature the random forest regression model was used with time series of LST (from Terra MODIS satellite collection 6) as a predictor variable. Monthly total precipitation data was obtained from CHIRPS version 2.0.

Seventeen bioclimatic variables derived from MODIS and CHIRPS data had a strong positive correlation with the WorldClim bioclimatic variables, and their frequency distributions were close. Two variables were the lower performance as annual mean diurnal range (02) and Isothermality (03) can be attributed to the fact that temperature extremes enter into their calculation. These temperature extremes are underestimated applying satellite-derived input data (Janatian et al., 2017; Duan et al., 2018; Hooker et al., 2018). As a consequence of the successful retrieval of the bioclimatic variables, we are confident that the estimated 19 bioclimatic variables will be very useful for a range of applications, in particular, if a higher spatial resolution is required such as for species distribution modeling.

The success of the modeling can be attributed to the fact that climatologies of both air temperature as well as precipitation can be well retrieved from EO data, in particular, if aggregated over monthly intervals and for regions such as Mongolia. In areas with sparse station density, EO data avoids otherwise necessary interpolation techniques.

The main limitation of many EO products relates to the fact that data sets are still relatively short (e.g. MODIS LST starting only in 2002) and that data from multiple satellites would have to be combined and normalized if longer time series are required. The advantage of the MODIS data set is, however, that it covers the most recent 15 years. For the future, spatial and temporal resolution, as well as spatial coverage, will favor EO data even more compared to other techniques as new satellites are launched at an unprecedented pace. For future research, we recommend to focusing on the improved quality, spatial, and temporal resolution of precipitation estimates.

Appendix

PERSIANN-CCS products obtained were downloaded from the CHRS Data Portal (available at CHRS Data Portal website) with a spatial resolution of 0.04°, covering Mongolia between 2003 and 2017. The PERSIANN algorithm focuses on the synergy between the sampled information from Low Earth Orbiting (LEO) satellites and the high-frequency samples from Geostationary (GEO) satellites which were developed at the Center for Hydrometeorology and Remote Sensing (CHRS) at the University of California, Irvine in 1997 (Nguyen et al., 2018). The PERSIANN-CCS algorithm uses additional information from the infrared cloud images by performing segmentation of the cloud image under different temperature thresholds.

Table A1 Summary statistics for monthly averages per climate region station-measured precipitation, CHIRPS and PERSIANN-CCS for the years 2003–2017. Each Köppen climate classification of Mongolia (Fig. 1(b)) is represented by weather stations

Köppen climate classification	Coefficient of determination (R^2)	
	Measured precipitation & CHIRPS	Measured precipitation & PERSIANN-CCS
BWk (Dalanzadgad)	0.989	0.389
BSk (Choir)	0.995	0.356
Dfc (Teshig)	0.984	0.013
Dsc (Khutag-Undur)	0.982	0.329
Dwb (Baruunturuun)	0.968	0.214
Dwc (Murun)	0.975	0.303
Dsb (Choibalsan)	0.972	0.302

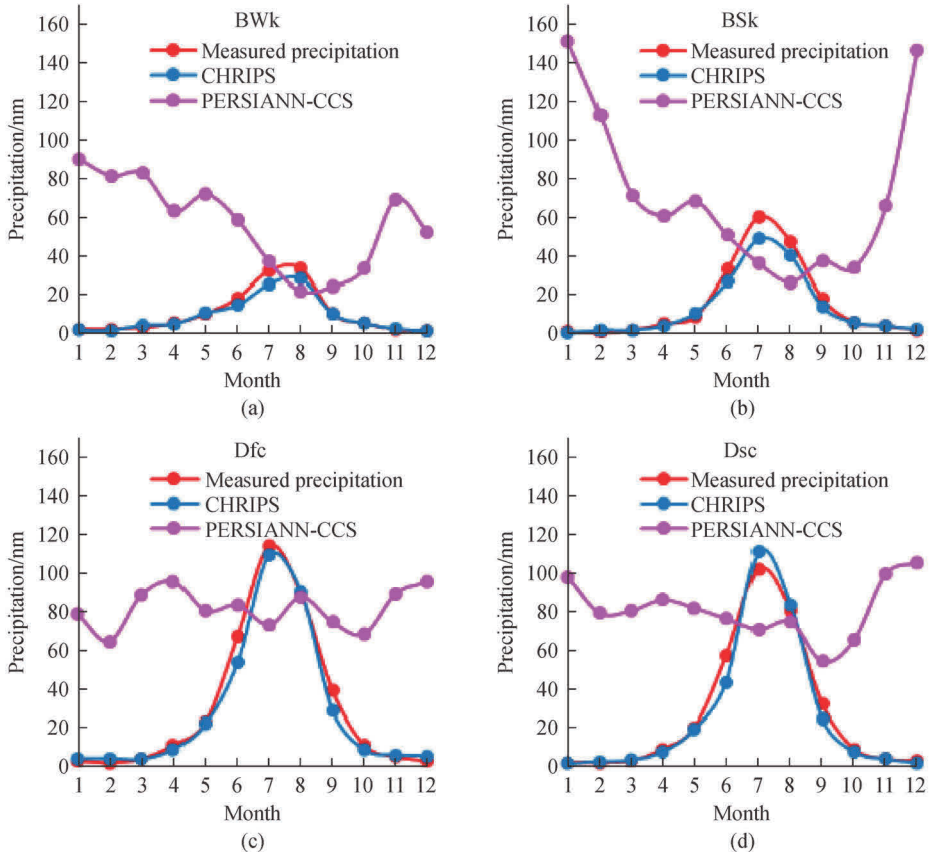

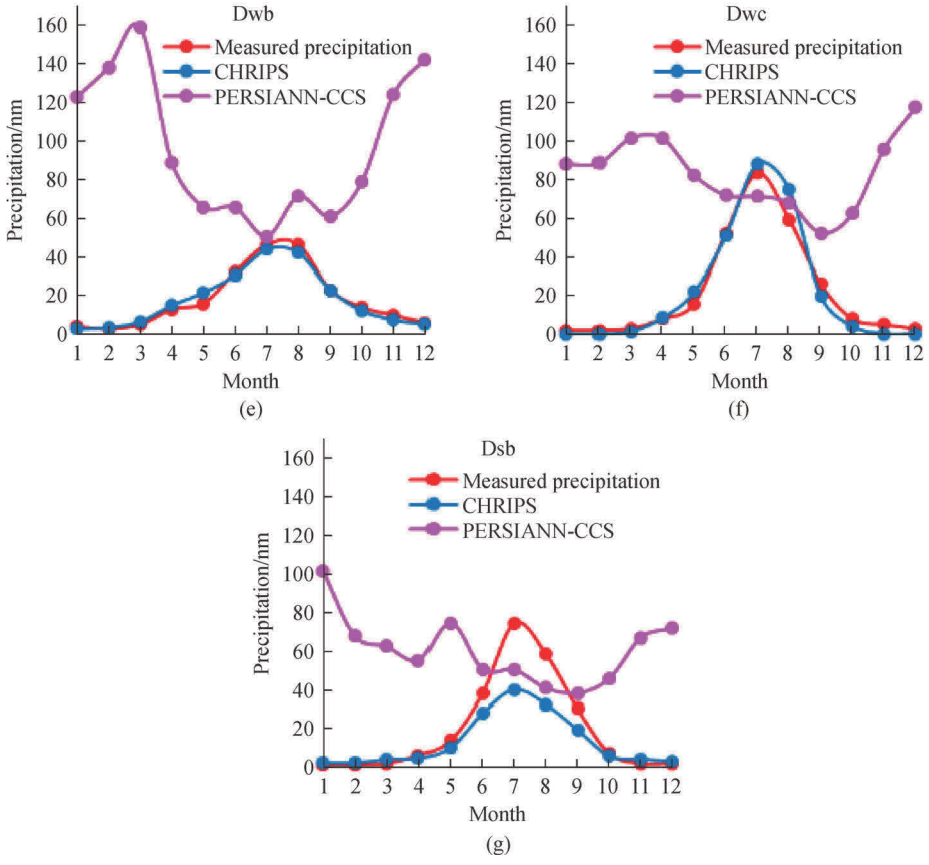

Fig. A1 Distribution of measured precipitation, CHIRPS, and PERSIANN-CCS times series (monthly data) for years 2002–2017.

Table A2 Descriptor statistics of the estimated monthly average, monthly minimum, monthly maximum air temperature, and monthly total precipitation for the years 2002–2017. T_{max}, T_{avg} and T_{min} are the monthly average, maximum and minimum air temperature, and *PPT* is the monthly total precipitation

Variables	Maximum	Mean	Minimum	Standard deviation
T_{max01}	−1.76	−14.39	−29.82	4.15
T_{max02}	0.02	−10.63	−26.47	4.30
T_{max03}	7.02	−2.95	−21.47	3.93
T_{max04}	17.04	5.75	−16.42	4.32
T_{max05}	27.68	16.43	−8.77	4.44
T_{max06}	30.89	21.14	−4.01	4.16
T_{max07}	32.33	22.13	−1.08	4.40
T_{max08}	29.77	19.82	−5.87	4.21
T_{max09}	23.51	12.84	−9.97	4.01
T_{max10}	13.26	3.52	−14.21	3.66
T_{max11}	4.10	−6.18	−18.14	3.40
T_{max12}	−0.21	−13.13	−25.91	3.20
T_{avg01}	−6.6	−20.83	−36.6	3.86
T_{avg02}	−0.6	−16.6	−35.1	3.98

(*Continued*)

Variables	Maximum	Mean	Minimum	Standard deviation
T_{avg03}	4.8	−6.73	−20.5	4.22
T_{avg04}	12.4	3.92	−7.6	3.32
T_{avg05}	19.3	10.75	2.8	3.05
T_{avg06}	24.9	16.98	9.2	3.06
T_{avg07}	27.2	19.49	11.6	3.21
T_{avg08}	25.6	17.16	8.7	3.34
T_{avg09}	19.7	10.48	2.6	3.12
T_{avg10}	11.7	1.49	−8.2	3.08
T_{avg11}	0.3	−9.62	−22.7	3.06
T_{avg12}	−6.1	−17.85	−31.5	3.05
T_{min01}	−11.77	−25.54	−39.76	4.21
T_{min02}	−6.01	−21.55	−36.16	4.50
T_{min03}	2.88	−9.94	−26.26	4.54
T_{min04}	11.14	1.02	−18.20	4.10
T_{min05}	19.26	8.08	−12.50	4.15
T_{min06}	25.52	14.86	−7.73	4.24
T_{min07}	28.77	17.56	−4.74	4.50
T_{min08}	26.86	15.20	−5.59	4.52
T_{min09}	17.80	7.24	−12.60	4.10
T_{min10}	9.27	−2.32	−20.36	4.00
T_{min11}	−0.31	−13.87	−28.04	4.04
T_{min12}	−7.21	−21.78	−35.07	3.98
PPT_{01}	20.02	2.19	0.00	1.91
PPT_{02}	18.35	2.29	0.00	1.65
PPT_{03}	25.47	3.33	0.00	1.49
PPT_{04}	48.00	7.19	0.00	3.85
PPT_{05}	77.61	14.80	0.26	7.62
PPT_{06}	125.51	33.24	1.58	19.06
PPT_{07}	197.70	52.56	9.12	28.54
PPT_{08}	189.36	47.65	2.44	23.58
PPT_{09}	92.34	17.20	0.51	9.55
PPT_{10}	59.95	7.34	0.00	4.36
PPT_{11}	48.34	4.28	0.00	2.74
PPT_{12}	44.56	3.02	0.00	1.88

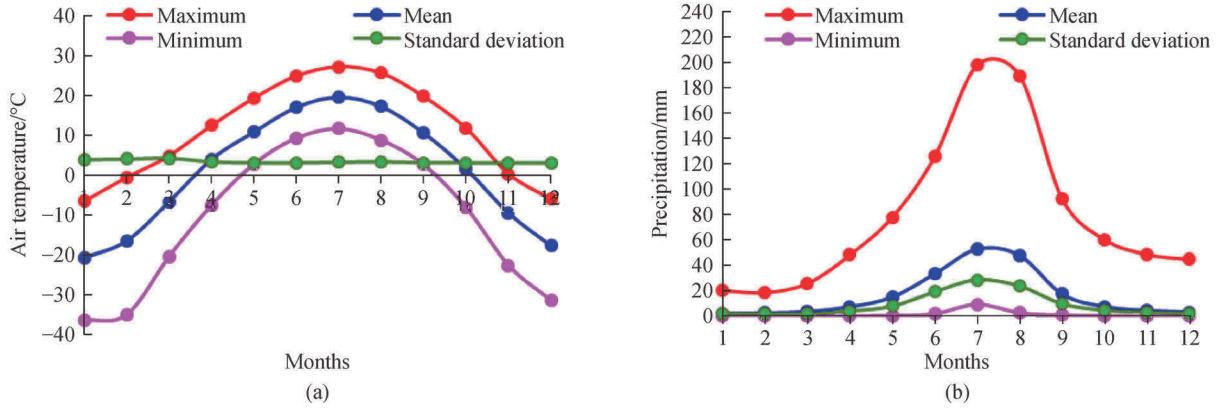

Fig. A2 Estimated monthly average temperature (a) derived from MODIS LST data, and monthly total precipitation retrieved from CHRIPS data (b) for the years 2002−2017.

Acknowledgements The authors appreciate the providers of temperature and precipitation products to allow us to download and use these data sets. We thank two anonymous referees for their comments on the manuscript.

References

Amiri M, Tarkesh M, Jafari R, Jetschke G (2020). Bioclimatic variables from precipitation and temperature records vs. remote sensing-based bioclimatic variables: Which side can perform better in species distribution modeling? Ecol Inform, 57: 101060

Anderson R P (2012). Harnessing the world's biodiversity data: promise and peril in ecological niche modeling of species distributions. Ann N Y Acad Sci, 1260(1): 66–80

Arriaga L, Castellanos A E, Moreno E, Alarcón J (2004). Potential ecological distribution of alien invasive species and risk assessment: a case study of buffel grass in arid regions of Mexico. Conserv Biol, 18(6): 1504–1514

Attorre F, Alfo M, De Sanctis M, Francesconi F, Bruno F (2007). Comparison of interpolation methods for mapping climatic and bioclimatic variables at regional scale. International Journal of Climatology, 27 (13): 1825–1843

Atzberger C, Rembold F (2013). Mapping the spatial distribution of winter crops at sub-pixel level using AVHRR NDVI time series and neural nets. Remote Sens, 5(3): 1335–1354

Bai P, Liu X (2018). Evaluation of five satellite-based precipitation products in two gauge-scarce basins on the Tibetan Plateau. Remote Sens, 10(8): 1316

Barzegar R, Adamowski J, Moghaddam A A (2016). Application of wavelet-artificial intelligence hybrid models for water quality prediction: a case study in Aji-Chay River, Iran. Stochastic Environmental Research and Risk Assessment, 30(7): 1797–1819

Beck H E, Van Dijk A I, Levizzani V, Schellekens J, Gonzalez Miralles D, Martens B, De Roo A (2017). MSWEP: 3-hourly 0.25 global gridded precipitation (1979–2015) by merging gauge, satellite, and reanalysis data. Hydrol Earth Syst Sci, 21(1): 589–615

Benali A, Carvalho A C, Nunes J P, Carvalhais N, Santos A (2012). Estimating air surface temperature in Portugal using MODIS LST data. Remote Sens Environ, 124: 108–121

Brown D P, Comrie A C (2002). Spatial modeling of winter temperature and precipitation in Arizona and New Mexico, USA. Clim Res, 22 (2): 115–128

Bryan B A, Crossman N D (2008). Systematic regional planning for multiple objective natural resource management. J Environ Manage, 88(4): 1175–1189

Dodson R, Marks D (1997). Daily air temperature interpolated at high spatial resolution over a large mountainous region. Clim Res, 8(1): 1–20

Duan S B, Li Z L, Wu H, Leng P, Gao M, Wang C (2018). Radiance-based validation of land surface temperature products derived from Collection 6 MODIS thermal infrared data. Int J Appl Earth Obs Geoinf, 70: 84–92

Erdenedalai A, Baast O, Tovuudorj R, Otgonbayar M, Bumtsend B, Tseveengerel B, Tuyagerel D, Munkhtur P, Sumiya E, Davaasuren D, Jigjidsuren S, Dorj D (2020). Landscape Ecological Potential of Mongolia. Ulaanbatar: Namnan Design Press (in Mongolian)

Feilhauer H, He K S, Rocchini D (2012). Modeling species distribution using niche-based proxies derived from composite bioclimatic variables and MODIS NDVI. Remote Sens, 4(7): 2057–2075

Fick S E, Hijmans R J (2017). WorldClim 2: new 1-km spatial resolution climate surfaces for global land areas. Int J Climatol, 37(12): 4302–4315

Franklin J (1995). Predictive vegetation mapping: geographic modelling of bio-spatial patterns in relation to environmental gradients. Prog Phys Geogr, 19(4): 474–499

Funk C, Verdin A, Michaelsen J, Peterson P, Pedreros D, Husak G (2015). A global satellite assisted precipitation climatology. Earth System Science Data Discussions, 8(1): 275–287

Hengl T, Walsh M G, Sanderman J, Wheeler I, Harrison S P, Prentice I C (2018). Global mapping of potential natural vegetation: an assessment of machine learning algorithms for estimating land potential. PeerJ, 6: e5457

Hijmans R J, Cameron S E, Parra J L, Jones P G, Jarvis A (2005). Very high resolution interpolated climate surfaces for global land areas. Int J Climatol, 25 (15): 1965–1978

Hooker J, Duveiller G, Cescatti A (2018). A global dataset of air

temperature derived from satellite remote sensing and weather stations. Sci Data, 5(1): 180246

Incerti G, Feoli E, Salvati L, Brunetti A, Giovacchini A (2007). Analysis of bioclimatic time series and their neural network-based classification to characterise drought risk patterns in South Italy. Int J Biometeorol, 51(4): 253–263

Janatian N, Sadeghi M, Sanaeinejad S H, Bakhshian E, Farid A, Hasheminia S M, Ghazanfari S (2017). A statistical framework for estimating air temperature using MODIS land surface temperature data. Int J Climatol, 37(3): 1181–1194

Kidd C, Levizzani V, Laviola S (2010). Quantitative precipitation estimation from Earth observation satellites. Rainfall. Stat Sci, 191: 127–158

Kottek M, Grieser J, Beck C, Rudolf B, Rubel F (2006). World map of the Köppen-Geiger climate classification updated. Meteorol Z (Berl), 15(3): 259–263

Kurtzman D, Kadmon R (1999). Mapping of temperature variables in Israel: comparison of different interpolation methods. Clim Res, 13 (1): 33–43

Lawrimore J H, Menne M J, Gleason B E, Williams C N, Wuertz D B, Vose R S, Rennie J (2011). An overview of the Global Historical Climatology Network monthly mean temperature data set, version 3. J Geophys Res D Atmospheres, 116(D19): 1–18

Leathwick J R, Overton J M, McLeod M (2003). An environmental domain classification of New Zealand and its use as a tool for biodiversity management. Conserv Biol, 17(6): 1612–1623

Li Z L, Tang B H, Wu H, Ren H, Yan G, Wan Z, Trigo I F, Sobrino J A (2013). Satellite-derived land surface temperature: current status and perspectives. Remote Sens Environ, 131: 14–37

Marchi M, Sinjur I, Bozzano M, Westergren M (2019). Evaluating WorldClim version 1 (1961–1990) as the baseline for sustainable use of forest and environmental resources in a changing climate. Sustainability, 11(11): 3043

Mesquita S, Sousa A J (2009). Bioclimatic mapping using geo-statistical approaches: application to mainland Portugal. Int J Climatol, 29 (14): 2156–2170

Nikolova N, Vassilev S (2006). Mapping precipitation variability using different interpolation methods. In: Proceedings of the conference on water observation and information system for decision support (BALWOIS), Bulgaria

Nguyen P, Ombadi M, Sorooshian S, Hsu K, AghaKouchak A, Braithwaite D, Thorstensen, A R (2018). The PERSIANN family of global satellite precipitation data: a review and evaluation of products. Hydrology and Earth System Sciences, 22(11), 5801–5816

O'Donnell M S, Ignizio D A (2012). Bioclimatic predictors for supporting ecological applications in the conterminous United States. US Geol Surv Data Ser, 691(10): 1–17

Olson D M, Dinerstein E, Wikramanayake E D, Burgess N D, Powell G V, Underwood E C, D'amico J A, Itoua I, Strand H E, Morrison J C, Loucks C J (2001). Terrestrial ecoregions of the world: a new map of life on earth a new global map of terrestrial ecoregions provides an innovative tool for conserving biodiversity. Bioscience, 51(11): 933–938

Otgonbayar M, Atzberger C, Mattiuzzi M, Erdenedalai A (2019). Estimation of climatologies of average monthly air temperature over Mongolia using MODIS Land Surface Temperature (LST) time series and machine learning techniques. Remote Sens, 11(21): 2588

Paredes-Trejo F J, Barbosa H A, Kumar T L (2017). Validating CHIRPS-based satellite precipitation estimates in Northeast Brazil. J Arid Environ, 139: 26–40

Peng C (2000). From static bio-geographical model to dynamic global vegetation model: a global perspective on modelling vegetation dynamics. Ecol Modell, 135(1): 33–54

Price K, Purucker S T, Kraemer S R, Babendreier J E, Knightes C D (2014). Comparison of radar and gauge precipitation data in watershed models across varying spatial and temporal scales. Hydrol Processes, 28(9): 3505–3520

Richter K, Hank T B, Mauser W, Atzberger C (2012). Derivation of biophysical variables from Earth observation data: validation and statistical measures. J Appl Remote Sens, 6(1): 063557

Ripley B D (2001). The R project in statistical computing. MSOR Connections. The newsletter of the LTSN Maths. Stats & OR Network, 1(1): 23–25

Robeson S M (1994). Influence of spatial sampling and interpolation on estimates of air temperature change. Clim Res, 4(2): 119–126

Roca R, Alexander L V, Potter G, Bador M, Jucá R, Contractor S, Bosilovich M G, Cloché S (2019). FROGS: a daily $1^{\circ} \times 1^{\circ}$ gridded precipitation database of rain gauge, satellite and reanalysis products. Earth Syst Sci Data, 11(3): 1017–1037

SAGA G (2013). System for automated geo-scientific analyses. Available at SAGA-GIS website

Salas E A L, Seamster V A, Boykin K G, Harings N M, Dixon K W (2017). Modeling the impacts of climate change on Species of Concern (birds) in South Central USA based on bioclimatic variables. AIMS Environ Sci, 4(2): 358

Sun Q, Miao C, Duan Q, Ashouri H, Sorooshian S, Hsu K L (2018). A review of global precipitation data sets: data sources, estimation, and intercomparisons. Rev Geophys, 56(1): 79–107

Sykes M T, Prentice I C, Cramer W (1996). A bioclimatic model for the potential distributions of north European tree species under present and future climates. Journal of Biogeography, 23, 203–233

Thompson R S, Shafer S L, Anderson K H, Strickland L E, Pelltier R T, Bartlein P J, Kerwin M W (2004). Topographic, bioclimatic, and vegetation characteristics of three ecoregion classification systems in North America: comparisons along continent-wide transects. Environ Manage, 34(Suppl 1): S125–S148

Title P O, Bemmels J B (2018). ENVIREM: an expanded set of bioclimatic and topographic variables increases flexibility and improves performance of ecological niche modeling. Ecography, 41(2): 291–307

Vancutsem C, Ceccato P, Dinku T, Connor S J (2010). Evaluation of MODIS land surface temperature data to estimate air temperature in different ecosystems over Africa. Remote Sens Environ, 114(2): 449–465

Vega G C, Pertierra L R, Olalla-Tárraga M Á (2017). MERRAclim, a high-resolution global dataset of remotely sensed bioclimatic variables for ecological modelling. Scientific Data, 4(1), 1–12

Vuolo F, Mattiuzzi M, Klisch A, Atzberger C (2012). Data service platform for MODIS Vegetation Indices time series processing at BOKU Vienna: current status and future perspectives. In: Earth Resources and Environmental Remote Sensing/GIS Applications III

(Vol. 8538): 85380A

Waltari E, Hijmans R J, Peterson A T, Nyári A S, Perkins S L, Guralnick R P (2007). Locating pleistocene refugia: comparing phylogeographic and ecological niche model predictions. PLoS One, 2(6): e563

Waltari E, Schroeder R, McDonald K, Anderson R P, Carnaval A (2014). Bioclimatic variables derived from remote sensing: assessment and application for species distribution modelling. Methods Ecol Evol, 5 (10): 1033–1042

Walther G R, Berger S, Sykes M T (2005). An ecological 'footprint' of climate change. Proc Biol Sci, 272(1571): 1427–1432

World Meteorological Organization (WMO) (2014). Climate Data Management System Specifications. Available at World Meteorological Organization website